

## Structure Determination of the $\text{Si}_3\text{N}_4/\text{Si}(111)$ -(8 × 8) Surface: A Combined Study of Kikuchi Electron Holography, Scanning Tunneling Microscopy, and *ab initio* Calculations

H. Ahn,<sup>1</sup> C.-L. Wu,<sup>1</sup> S. Gwo,<sup>1</sup> C. M. Wei,<sup>2</sup> and Y. C. Chou<sup>1</sup>

<sup>1</sup>*Department of Physics, National Tsing-Hua University, Hsinchu, Taiwan 300, Republic of China*

<sup>2</sup>*Institute of Physics, Academia Sinica, Nankang, Taipei, Taiwan 115, Republic of China*

(Received 23 October 2000)

A comprehensive atomic model for the reconstructed surface of  $\text{Si}_3\text{N}_4$  thin layer grown on  $\text{Si}(111)$  is presented. Kikuchi electron holography images clearly show the existence of adatoms on the  $\text{Si}_3\text{N}_4(0001)/\text{Si}(111)$ -(8 × 8) surface. Compared with the *ab initio* calculations, more than 30 symmetry-inequivalent atomic pairs in the outmost layers are successfully identified. Scanning tunneling microscopy (STM) images show diamond-shaped unit cells and nine adatoms in each cell. High-resolution STM images reveal extra features and are in good agreement with the partial charge density distribution obtained from total-energy calculations.

DOI: 10.1103/PhysRevLett.86.2818

PACS numbers: 61.14.Nm, 61.50.Ah, 68.37.Ef, 77.55.+f

Silicon nitride ( $\text{Si}_3\text{N}_4$ ) film has been widely used for high-temperature ceramic and microelectronic applications due to its unique properties. Recently, as the scaling of ultralarge-scale integrated circuits continues into the nanometer regime to achieve high levels of integration and speed, ultrathin  $\text{Si}_3\text{N}_4$  and silicon oxynitride ( $\text{SiO}_x\text{N}_y$ ) films have become increasingly important for replacing silicon dioxide ( $\text{SiO}_2$ ) as the gate dielectric material [1]. At present, the structural and electronic properties of  $\text{Si}_3\text{N}_4$  films grown on Si are the subjects of many theoretical [2] and experimental [3] papers.

$\text{Si}_3\text{N}_4$  films deposited on Si are usually amorphous. However, as an exception, a coherent  $\text{Si}_3\text{N}_4(0001)/\text{Si}(111)$  interface can be formed using the thermal nitridation process, where a Si substrate is exposed to various nitrogen-containing gases such as  $\text{NH}_3$  [4–6],  $\text{NO}$  [7–9], and  $\text{N}_2$  [10], or to N atom [11] or ion [12] beams at high substrate temperatures. This is related to a nearly perfect lattice match: The  $2 \times 2$  cell of the  $\text{Si}(111)$  surface ( $a_{\text{Si}} = 3.84 \text{ \AA}$ ) is only  $\sim 1.1\%$  bigger than the unit cell of  $\beta\text{-Si}_3\text{N}_4(0001)$  ( $a_{\beta\text{-Si}_3\text{N}_4} = 7.61 \text{ \AA}$ ) [13]. Indeed, the ordered  $8 \times 8$  surface superstructure of  $\text{Si}_3\text{N}_4/\text{Si}(111)$  has been first reported by low-energy electron diffraction (LEED) studies [4,11]. In the later scanning tunneling microscopy (STM) studies [5,8,10], however, only a  $\sim 10.2 \times 10.2 \text{ \AA}^2$  (so-called  $\frac{8}{3} \times \frac{8}{3}$ ) structure is observed. Several contradicting structural models have been proposed so far for the intriguing  $\text{Si}_3\text{N}_4(0001)/\text{Si}(111)$ -(8 × 8) surface, although none of them are conclusive [5–7,10].

In this Letter, a structural model is proposed by a combined study of Kikuchi electron holography (KEH), STM, and *ab initio* total-energy calculations. The observation of the adatoms with  $\sim 10 \text{ \AA}$  separation in the first atomic layer of the surface by KEH plays a key role in the determination of the structure. The clear diamond-shaped unit cells including nine adatoms were observed in the occupied-state STM images. With the nitrogen adatoms and the  $\text{Si}_3\text{N}_4$

rest layer on the  $\text{Si}(111)$  substrate as the starting model, we performed the energy minimization processes with *ab initio* calculations. The partial charge density distribution of our final structure shows a good correspondence with the STM images. Scanning tunneling spectroscopy (STS) was also used to measure the energy position of the observed occupied states in the STM images of adatoms. We found a peak at 4.2 eV below the Fermi level, which is consistent with the reported energy position of dangling N-2*p* electrons in the ultraviolet photoelectron spectroscopy (UPS) spectra [14,15], indicating that the observed adatoms are nitrogen atoms.

A sharp and well-ordered  $8 \times 8$  LEED pattern was observed when the clean  $\text{Si}(111)$ -(7 × 7) sample reacts with  $\text{NH}_3$  gas at the temperature above 1100 K. The three-dimensional structural information was reconstructed in a holographic inversion scheme by a Fourier transform of the Kikuchi patterns. To remove the artifact caused by the multiple scattering effects, we have measured a series of Kikuchi patterns at the beam energy between 78 and 340 eV and used the integral-energy phase-summing method developed by Wei and Tong [16]. The details of the KEH method are well described in our previous papers [17]. STM images were acquired with a commercial (Omicron) STM system. Normalized tunneling spectra [ $(dI/dV)/(I/V)$ ] were acquired with simultaneous measurements of  $dI/dV$ - $V$  (using a lock-in amplifier) and  $I$ - $V$  curves, while temporarily opening the constant-current feedback loop.

Based on the three experimental facts we found in KEH and STM studies, we propose a new atomic model of  $8 \times 8$  surface structure. The first fact has come from the off-normal KEH images. Figure 1 shows the reconstructed images using KEH study at  $z = 0 \text{ \AA}$  (which means that the emitters and the scatters are in the same atomic plane) for three glancing angles of incidence ( $30^\circ$ ,  $60^\circ$ , and  $70^\circ$ ) along the  $[11\bar{2}]$  direction. The brightest reconstructed image spots (3) marked with circles in Figs. 1(b) and 1(c)

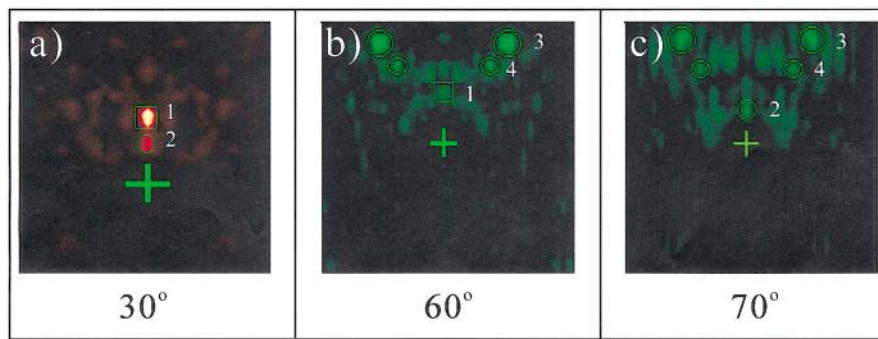


FIG. 1 (color). The atomic images reconstructed from KEH patterns at  $z = 0 \text{ \AA}$  for the incident angles of (a)  $30^\circ$ , (b)  $60^\circ$ , and (c)  $70^\circ$ . The cross marks the position of an emitter.

appeared at  $[5.0, 8.2, -0.5] (\text{\AA})$  and  $[5.5, 8.7, 0.0] (\text{\AA})$ , respectively. There is no similar atomic pair in smaller incidence angle KEH, for example,  $30^\circ$  in Fig. 1(a). Therefore the atomic pairs we found at  $60^\circ$  and  $70^\circ$  are mostly originated from the surface. The distance between the emitter to the scatterer of the image spot 3 is about  $10 \text{ \AA}$ . This distance is very close to the periodicity of the  $\frac{8}{3} \times \frac{8}{3}$  structure observed for many previous papers [5,8,10]. Meanwhile, in the original LEED patterns, the three-eighth fractional index spots are always much brighter [6,11] than the others and persist as long as there is  $8 \times 8$  surface structure. Therefore, this superstructure of adatoms is intrinsic, so does not depend on the purity of  $\text{NH}_3$  gas or the preparation conditions as mentioned by Wang *et al.* [6].

The second fact can be found in Fig. 2(a), where we show the occupied-state STM image of an  $8 \times 8$  surface taken at  $V_s = -4 \text{ V}$  and  $I_t = 0.5 \text{ nA}$ . Under these scanning conditions, we can observe not only the  $\frac{8}{3} \times \frac{8}{3}$  structure but also the  $8 \times 8$  diamond-shaped unit cell with clear boundary. The side length of the diamond-shaped cell is about  $31 \text{ \AA}$ , which is believed to be responsible for the formation of  $8 \times 8$  ( $= 3.84 \text{ \AA} \times 8$ ) LEED pattern. For the  $8 \times 8$  surface, we need a high sample bias voltage ( $\approx -4 \text{ V}$ ) for atomic-resolution images, while the  $(7 \times 7)$ -reconstructed Si(111) surface could be imaged using a low sample bias because of its metallic character. The STS measurements  $[(dI/dV)/(I/V)]$  displayed in Fig. 2(b) were taken on the  $8 \times 8$  nitride surface and the Si(111)- $(7 \times 7)$  surface before nitridation. In contrast to many Si dangling bond states observed on the Si(111)- $(7 \times 7)$  surface (i.e., adatom dangling states and back-bond state) [18], only a prominent occupied surface state is observed at  $\sim -4.2 \text{ eV}$  below the Fermi level on the  $8 \times 8$  surface, consistent with the STM imaging conditions. The measured band gap on the  $8 \times 8$  surface is about  $4\text{--}5 \text{ eV}$ , in good agreement with the calculated indirect band gap of  $\beta\text{-Si}_3\text{N}_4$  [13]. These results indicate that the occupied-state STM image corresponds to the spatial locations of the electronic state at  $-4.2 \text{ eV}$ , and this state is completely different from the observed Si dangling states on the bare  $7 \times 7$  surface. Interestingly, previous UPS studies [14] have identified this state as the dangling N- $2p$  state, and it could be resolved only when the nitrided

surface was annealed to the high temperature ( $\sim 1100 \text{ K}$ ) required to form the  $8 \times 8$  ordering. The identification of N- $2p$  has also been confirmed theoretically [15]. Therefore, from the STS results, we conclude that the  $\frac{8}{3} \times \frac{8}{3}$

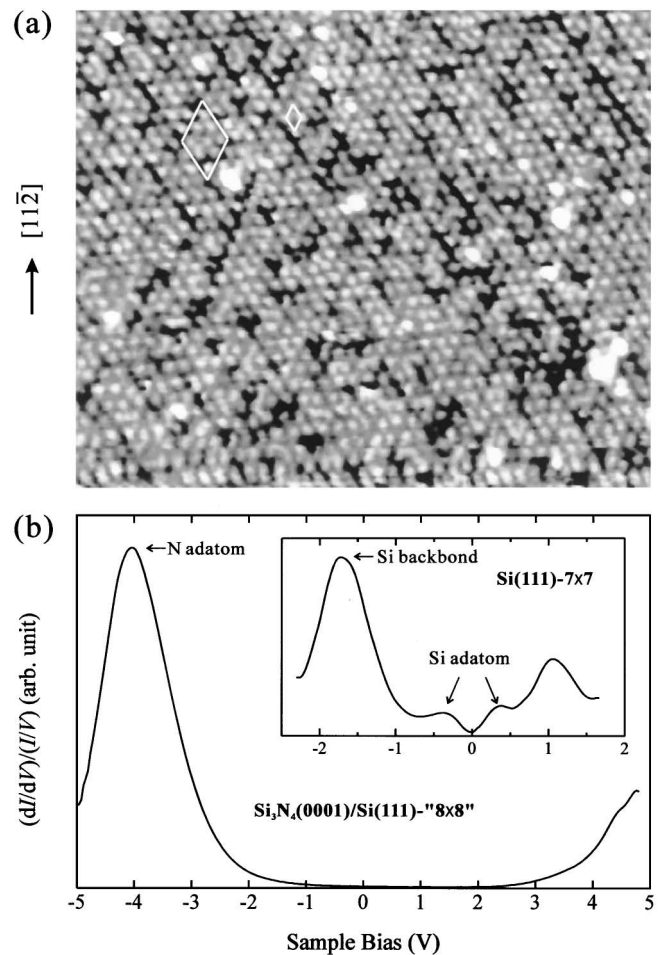


FIG. 2. (a) Occupied-state STM image ( $V_s = -4.0 \text{ V}$ ,  $I_t = 1.0 \text{ nA}$ ) on the  $(8 \times 8)$ -reconstructed  $\text{Si}_3\text{N}_4(0001)/\text{Si}(111)$  surface prepared by exposing a Si(111) substrate to back-filled  $\text{NH}_3$  gas ( $1 \times 10^{-8} \text{ Torr}$  for  $20 \text{ min} \equiv 12 \text{ L}$ ) at  $1173 \text{ K}$  sample temperature. Both  $8 \times 8$  and  $\frac{8}{3} \times \frac{8}{3}$  cells are outlined. Note that there are many dislocated  $8 \times 8$  cells on the surface. (b) Typical normalized tunneling spectrum  $[(dI/dV)/(I/V)]$  taken on the  $8 \times 8$  nitride surface. Inset shows a spectrum acquired on the bare Si(111)- $(7 \times 7)$  surface.

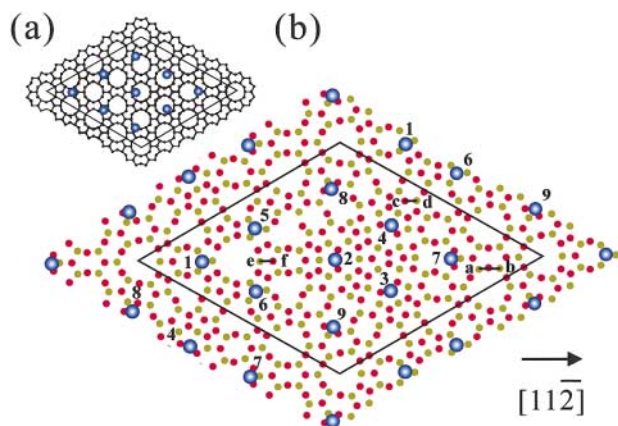


FIG. 3 (color). The proposed  $8 \times 8$  atomic model before (a) and after (b) the total energy relaxation. The large blue solid circles in (a) and (b) are nitrogen adatoms on the topmost layer. The small red (green) solid circles are nitrogen (silicon) atoms on the rest layer.

ordering spots in the occupied state images correspond to the nitrogen adatoms.

For all of our KEH measurements, the incident electron beam follows the  $[11\bar{2}]$  direction of the Si(111) substrate, and all of the reconstructed atomic pairs including those in Fig. 1 appeared symmetric along this direction. This fact suggests that  $\text{Si}_3\text{N}_4$  rest layer has a mirror symmetry about the  $[11\bar{2}]$  direction of the Si(111) substrate. Indeed, the LEED patterns about the  $[11\bar{2}]$  direction show mirror symmetry as well as threefold rotational symmetry. The possibility of multiple-domain averaging effects can be ruled out since large-area STM images in our experiments support the formation of single-domain  $8 \times 8$  surface. These results provide us the third reason to seek a new atomic structure model of the  $8 \times 8$  surface.

The proposed atomic model is similar to the Si(111)- $(7 \times 7)$  model, which consists of an upper adatom layer which caps the rest layer beneath. The rest layer before relaxation has  $1 \times 1$  unit cell of  $\text{Si}_3\text{N}_4$  as shown in Fig. 3(a). Repeated  $1 \times 1$  unit cells form the circular feature, which has three high-level nitrogen atoms and three low-level nitrogen atoms on the alternative corner of a circle. On top of this rest layer, we include the nitrogen adatoms with the periodicity of  $10.2 \text{ \AA}$ , as suggested by the KEH images, and performed *ab initio* total-energy calculations using the Vienna *ab initio* simulation package [19]. Until now, no total-energy calculations for this surface structure have been attempted because of the extreme difficulty of handling such a large number of two different kinds of atoms. For this calculation, we build a model using one layer of N adatoms, one rest layer of  $\beta\text{-Si}_3\text{N}_4(0001)$ , and a two-bilayer substrate of Si(111). The structure includes 137 N atoms (nine of them are adatoms) and 224 Si atoms in the  $8 \times 8$  relaxed layer, 128 Si atoms in the Si(111)  $1 \times 1$  substrate, and 64 H atoms were used to saturate the bottom Si dangling bonds.

Figure 3(b) shows the atomic structure of the adatom layer and the rest layer after the total-energy calculations

TABLE I. The comparison of the reconstructed atomic pairs identified in Fig. 1 with the theoretically expected position from the *ab initio* calculations of our model.

Spots	Reconstructed atomic pairs from KEH ( $\text{\AA}$ )	Assigned pairs	Ideal coordinates from our model ( $\text{\AA}$ )
1	$(0, 2.74, -0.82)$	<i>a-b</i>	$(0, 2.79, -1.2)$
2	$(0, 1.64, -0.85)$	<i>c-d</i> <i>e-f</i>	$(0, 1.55, -0.68)$ $(0, 1.46, -1.1)$
3	$(5.0, 8.2, -0.5)$ $[60^\circ]$ $(5.5, 8.7, 0.0)$ $[70^\circ]$	8-4	$(4.6, 7.7, -0.5)$
4	$(3.84, 6.5, 0.5)$ $[60^\circ]$ $(3.84, 6.0, 0.5)$ $[70^\circ]$	1-6	$(3.9, 6.8, 0.0)$

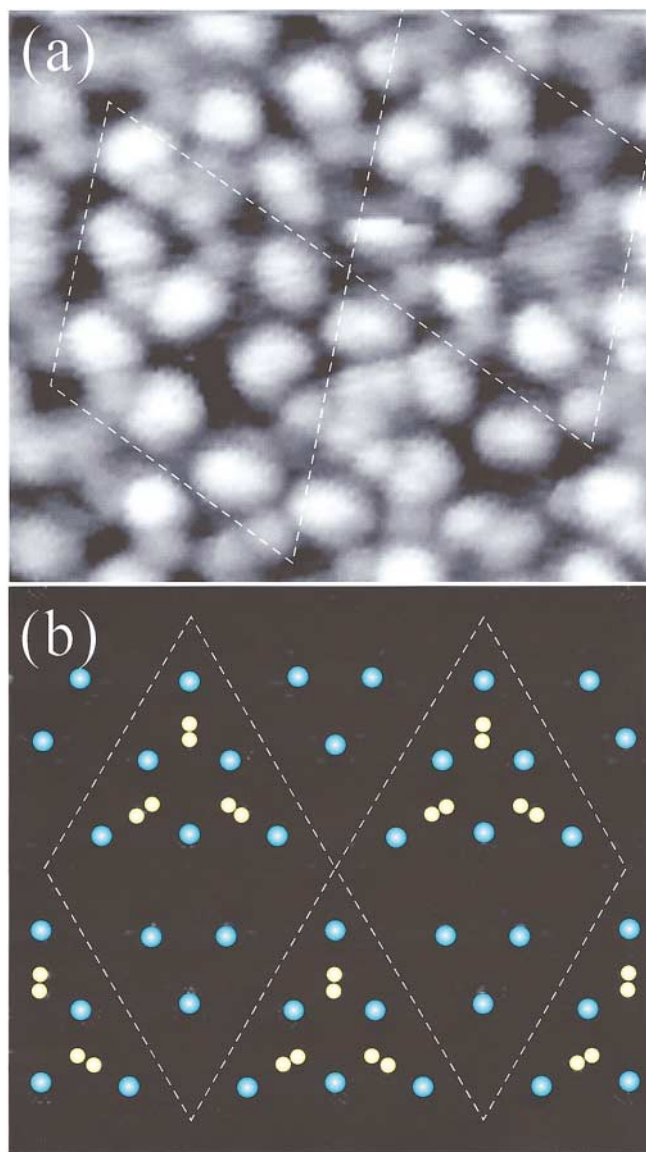


FIG. 4 (color). (a) High-resolution STM image taken at  $V_s = -4.0 \text{ V}$  and  $I_t = 1.0 \text{ nA}$ . (b) Calculated partial charge distribution of the outermost plane. Dashed diamond (smaller than the unit cell) is used as the guidance to show nine adatoms in a unit cell.

with adatoms. To avoid the complexity, we omitted displaying Si(111) substrate. The green and red solid circles are silicon and nitrogen atoms, respectively, and blue solid circles mark adatoms. As one can see in the left half of the diamond unit cell, three adatoms (1, 5, and 6) that lie on the top site of tetrahedral bonding in the rest layer do not disturb the basic feature of the underneath rest layer. However, in the right half of the unit cell, the adatoms sit approximately on the hollow site of the rest layer and have atomic bonds with two nitrogen atoms. The rest layer structure near these adatoms is extremely distorted. This uneven relaxation around adatoms results in the formation of a big diamond-shaped unit cell and the asymmetry of the left and right half of the unit cell. One unit cell is marked with the solid line. In this figure, each cell has the mirror symmetry axis along the long diagonal axis of the diamond as well as threefold rotational symmetry.

Compared with the atomic coordinates in our model, the atomic image spot 3 observed in Fig. 1 can be identified as the atomic pairs between adatoms (8-4) pair with the coordinate at  $[4.6, 7.7, -0.5]$  (Å). The atomic image spot 4 at  $[3.8, 6.5, 0.5]$  in Figs. 1(b) and 1(c) can be assigned to the atomic pair between adatoms (1-6) with the coordinate at  $[3.9, 6.8, 0.0]$  (Å). The weak features in Fig. 1 can also be assigned to the atomic pairs in our model. Within the accuracy of KEH, the agreement is very good. Table I shows the atomic pairs found in Fig. 1 along with the expected values from the *ab initio* calculations.

The high-resolution STM image ( $80 \times 70 \text{ \AA}^2$ ) taken at  $V_s = -4.0 \text{ V}$  and  $I_t = 1.0 \text{ nA}$ , as shown in Fig. 4(a), displays an interesting feature of the surface. In the upper half of a diamond unit cell, there are three additional bright spots next to the adatoms and these six spots form a hexagon feature. To directly compare STM images with our model, we calculated partial-charge-density distribution (PCD) of our model. The results shown in Fig. 4(b) present clearly separated diamond-shaped unit cells including nine adatoms (blue circles) as we observed in Fig. 2. Meanwhile, in the upper part of each unit cell, there are three additional paired atoms (yellow circles) between adatoms, which is a unique feature that appeared only in the PCD result. These paired atoms belong to the rest layer, but have a similar electronic status with the adatoms. If we consider that these paired spots can be imaged as only one spot within the resolution of STM, high-resolution STM images in Fig. 4(a) show an excellent correspondence with our PCD results. Recently, Morita *et al.* also observed this hexagon feature in their high-resolution STM study [10].

More than 30 reconstructed atomic pairs were successfully assigned compared with the theoretical results. The detailed list of the atomic pair comparison and the model description will be published elsewhere. The image spot 2 in Fig. 1(a), which locates at  $[0.0, 1.64, -0.85]$  (Å) can be compared with the Si-N atomic pairs with tetrahedral bond, such as (c-d)  $[0, 1.55, -0.68]$  (Å) or (e-f)  $[0, 1.46, -1.1]$  (Å). We can calculate the Si-N tetrahedral

atomic bond length from these pairs, which is the most prevailing pair in the rest layer. The calculated bond length is 1.70–1.83 Å, which is in excellent agreement with the previously reported results, 1.68–1.78 Å [7,20].

In summary, we have proposed a new atomic model of the  $\text{Si}_3\text{N}_4(0001)/\text{Si}(111)-(8 \times 8)$  surface based on the experimental results from KEH, STM, and STS measurements. We demonstrate, for the first time, the existence of the  $\frac{8}{3} \times \frac{8}{3}$ -ordered nitrogen adatoms on the top layer and the  $8 \times 8$  diamond-shaped unit cells in the real space. This proposed model is in good agreement with the *ab initio* total-energy calculations.

We acknowledge National Center for High-Performance Computing, Hsinchu, Taiwan, for the computer time. This work was partly supported by the National Science Council, Republic of China, and the Program for Promoting Academic Excellence of Universities, the Ministry of Education, Taiwan, Republic of China.

- 
- [1] *Fundamental Aspects of Ultrathin Dielectrics on Si-Based Devices*, edited by E. Garfunkel, E. P. Gusev, and A. Vul' (Kluwer Academic Publishers, Dordrecht, 1998).
  - [2] A. Omeltchenko *et al.*, Phys. Rev. Lett. **84**, 318 (2000); M. E. Bachlechner *et al.*, Phys. Rev. Lett. **84**, 322 (2000).
  - [3] C. Meyer *et al.*, Phys. Rev. Lett. **74**, 3001 (1995).
  - [4] A. J. van Bommel and E. Meyer, Surf. Sci. **8**, 381 (1967).
  - [5] E. Bauer *et al.*, Phys. Rev. B **51**, 17891 (1995).
  - [6] X.-S. Wang *et al.*, Phys. Rev. B **60**, R2146 (1999).
  - [7] M. Nishijima *et al.*, Surf. Sci. **137**, 473 (1984).
  - [8] B. Röttger, R. Kliese, and H. Neddermeyer, J. Vac. Sci. Technol. B **14**, 1051 (1996).
  - [9] M. D. Wiggins, R. J. Baird, and P. Wynblatt, J. Vac. Sci. Technol. **18**, 965 (1981); Ph. Avouris and R. Wolkow, Phys. Rev. B **39**, 5091 (1989).
  - [10] Y. Morita and H. Tokumoto, Surf. Sci. **443**, L1037 (1999).
  - [11] A. G. Schrott and S. C. Fain, Jr., Surf. Sci. **111**, 39 (1981); **123**, 204 (1982).
  - [12] J. S. Ha *et al.*, Appl. Phys. A **66**, S495 (1998).
  - [13] A. Y. Liu and M. L. Cohen, Phys. Rev. B **41**, 10727 (1990); Y.-N. Xu and W. Y. Ching, Phys. Rev. B **51**, 17379 (1995).
  - [14] T. Isu and K. Fujiwara, Solid State Commun. **42**, 477 (1982); F. Bozso and Ph. Avouris, Phys. Rev. B **38**, 3937 (1988); G. Dufour *et al.*, Surf. Sci. **304**, 33 (1994).
  - [15] J. Robertson, Philos. Mag. B **44**, 215 (1981); J. Appl. Phys. **54**, 4490 (1983); R.-H. Zhou, P.-L. Cao, and S.-B. Fu, Surf. Sci. **249**, 129 (1991).
  - [16] C. M. Wei and S. Y. Tong, Surf. Sci. **274**, L577 (1992).
  - [17] C. Y. Chang *et al.*, Phys. Rev. B **59**, R10453 (1999); T.-S. Shen *et al.*, Surf. Rev. Lett. **6**, 97 (1999).
  - [18] R. Losio *et al.*, Phys. Rev. B **61**, 10845 (2000).
  - [19] G. Kress and J. Hafner, Phys. Rev. B **47**, 558 (1993); **49**, 14251 (1994); G. Kress and J. Hafner, J. Phys. Condens. Matter **6**, 8245 (1994).
  - [20] G. L. Zhao and M. E. Bachlechner, Phys. Rev. B **58**, 1887 (1998); H. Wang *et al.*, Surf. Sci. **443**, L1037 (1999).